

Cavity-Q Aging Observed via an Atomic-Candle Signal

30 April 2004

Prepared by

J. G. COFFER, B. SICKMILLER, and J. C. CAMPARO
Electronics and Photonics Laboratory
Laboratory Operations

Prepared for

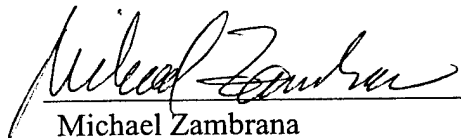
SPACE AND MISSILE SYSTEMS CENTER
AIR FORCE SPACE COMMAND
2430 E. El Segundo Boulevard
Los Angeles Air Force Base, CA 90245

Engineering and Technology Group

This report was submitted by The Aerospace Corporation, El Segundo, CA 90245-4691, under Contract No. FA8802-04-C-0001 with the Space and Missile Systems Center, 2430 E. El Segundo Blvd., Los Angeles Air Force Base, CA 90245. It was reviewed and approved for The Aerospace Corporation by B. Jaduszliwer, Principal Director, Electronics and Photonics Laboratory. Michael Zambrana was the project officer for the Mission-Oriented Investigation and Experimentation (MOIE) program.

This report has been reviewed by the Public Affairs Office (PAS) and is releasable to the National Technical Information Service (NTIS). At NTIS, it will be available to the general public, including foreign nationals.

This technical report has been reviewed and is approved for publication. Publication of this report does not constitute Air Force approval of the report's findings or conclusions. It is published only for the exchange and stimulation of ideas.



Michael Zambrana
SMC/AXE

REPORT DOCUMENTATION PAGE			Form Approved OMB No. 0704-0188	
<small>Public reporting burden for this collection of information is estimated to average 1 hour per response, including the time for reviewing instructions, searching existing data sources, gathering and maintaining the data needed, and completing and reviewing this collection of information. Send comments regarding this burden estimate or any other aspect of this collection of information, including suggestions for reducing this burden to Department of Defense, Washington Headquarters Services, Directorate for Information Operations and Reports (0704-0188), 1215 Jefferson Davis Highway, Suite 1204, Arlington, VA 22202-4302. Respondents should be aware that notwithstanding any other provision of law, no person shall be subject to any penalty for failing to comply with a collection of information if it does not display a currently valid OMB control number. PLEASE DO NOT RETURN YOUR FORM TO THE ABOVE ADDRESS.</small>				
1. REPORT DATE (DD-MM-YYYY) 30-04-2004		2. REPORT TYPE		3. DATES COVERED (From - To)
4. TITLE AND SUBTITLE Cavity-Q Aging Observed via an Atomic-Candle Signal		5a. CONTRACT NUMBER FA8802-04-C-0001		
		5b. GRANT NUMBER		
		5c. PROGRAM ELEMENT NUMBER		
6. AUTHOR(S) J. G. Coffey, B. Sickmiller, and J. C. Camparo		5d. PROJECT NUMBER		
		5e. TASK NUMBER		
		5f. WORK UNIT NUMBER		
7. PERFORMING ORGANIZATION NAME(S) AND ADDRESS(ES) The Aerospace Corporation Laboratory Operations El Segundo, CA 90245-4691		8. PERFORMING ORGANIZATION REPORT NUMBER TR-2004(8555)-4		
9. SPONSORING / MONITORING AGENCY NAME(S) AND ADDRESS(ES) Space and Missile Systems Center Air Force Space Command 2450 E. El Segundo Blvd. Los Angeles Air Force Base, CA 90245		10. SPONSOR/MONITOR'S ACRONYM(S) SMC		
		11. SPONSOR/MONITOR'S REPORT NUMBER(S) SMC-TR-04-14		
12. DISTRIBUTION/AVAILABILITY STATEMENT Approved for public release; distribution unlimited.				
13. SUPPLEMENTARY NOTES				
14. ABSTRACT Slow variations in cavity-Q and microwave power are thought to play a role in the long-term frequency stability of gas-cell atomic clocks. Here, we use an atomic-candle method to study the aging of a TE_{011} microwave cavity's resonant frequency and quality factor when a glass resonance cell containing Rb^{87} loads the cavity. Our results suggest that the alkali vapor coats the inside glass surface of the resonance cell with a thin metallic film; and that, as this film evolves, the quality factor degrades. (In our experiments, the quality factor changed by 30% over a timescale of months.) More generally, the present work demonstrates the efficacy of the atomic-candle method for investigating cavity resonances. In particular, we show that, when used in conjunction with more traditional methods, the atomic-candle method has the potential to reveal information on a cavity mode's spatial profile.				
15. SUBJECT TERMS				
16. SECURITY CLASSIFICATION OF:			17. LIMITATION OF ABSTRACT	18. NUMBER OF PAGES 7
a. REPORT UNCLASSIFIED	b. ABSTRACT UNCLASSIFIED	c. THIS PAGE UNCLASSIFIED		
				19a. NAME OF RESPONSIBLE PERSON James Camparo
				19b. TELEPHONE NUMBER (include area code) (310)336-6944

Note

The material reproduced in this report originally appeared in *IEEE Transactions on Ultrasonics*. The TR is published to document the work for the corporate record.

Cavity-Q Aging Observed via an Atomic-Candle Signal

John G. Coffer, Brett Sickmiller, and James C. Camparo

Abstract—Slow variations in cavity-Q and microwave power are thought to play a role in the long-term frequency stability of gas-cell atomic clocks. Here, we use an atomic-candle method to study the aging of a TE_{011} microwave cavity's resonant frequency and quality factor when a glass resonance cell containing Rb^{87} loads the cavity. Our results suggest that the alkali vapor coats the inside glass surface of the resonance cell with a thin metallic film; and that, as this film evolves, the quality factor degrades. (In our experiments the quality factor changed by $\sim 30\%$ over a timescale of months.) More generally, the present work demonstrates the efficacy of the atomic-candle method for investigating cavity resonances. In particular, we show that, when used in conjunction with more traditional methods, the atomic-candle method has the potential to reveal information on a cavity mode's spatial profile.

I. INTRODUCTION

THOUGH documented, it is not always appreciated that the gas-cell atomic clock's output frequency depends on the electrical characteristics of the clock's microwave cavity, specifically the cavity's resonant frequency, ω_c , and quality factor, Q_c . Two mechanisms are primarily responsible for this sensitivity, the position-shift effect [1], [2] and a cavity-pulling effect [3]. As a consequence, since the late 1980s there have been suggestions that the long-term stability of gas-cell clocks might be influenced by the microwave cavity [4], [5]. Therefore, it comes as a surprise to find a dearth of studies in the open literature dealing with this issue. Although some authors have considered the magnitude of the cavity-pulling effect [6], [7], and others have considered the design of compact, dielectrically loaded cavities for miniaturized devices [8]–[10], we know of no studies addressing potential deterministic/stochastic variations of either ω_c or Q_c in the gas-cell clock. Of course, it is well-known that, for an unloaded microwave cavity, ω_c will change in response to the cavity's temperature, primarily as a result of thermal expansion [11]. However, in the case of gas-cell clocks, a glass resonance cell loads the microwave cavity. Because the resonance cell contains an alkali vapor, the cell's inside surface will become coated with a thin conducting metallic film [12], and this could lead to a non-negligible increase in the rate at which modal

field energy is lost. Consequently, one could easily imagine the loaded cavity's resonant frequency and quality factor changing as a rubidium film slowly evolved on the resonance cell's inner surface.

In this work, we describe experiments examining the temporal behavior of a microwave cavity's resonant frequency and quality factor when loaded by an alkali-containing glass resonance cell. To this end, we have taken advantage of the atoms' atomic-candle signal [13], which is an atomic measure of microwave field strength [14]. With our atomic-candle method we are able to probe the field inside the cavity at the location in which the atoms generate the atomic clock signal (i.e., we perform a local measurement of field strength). In more standard techniques for studying cavity resonances (e.g., transmitted power methods [15]), global cavity field strength is measured. In Section II we describe the atomic-candle signal and our experimental method. In Section III, we report on the long-term aging of ω_c and Q_c due to what we hypothesize is a redistribution of rubidium metal within the resonance cell. We conclude with a discussion of the atomic clock stability issues raised by our findings.

II. ATOMIC-CANDLE METHOD FOR MEASURING A CAVITY'S RESONANCE

Over the past decade, researchers have come to recognize that atomic systems can exhibit parametric or Rabi-resonances [16], [17], in which this particular type of resonant behavior arises from an atom's interaction with a modulated field. Briefly, the modulated field induces atomic population oscillations, and the amplitude of these oscillations, δ_{pop} , exhibits resonance when the field's modulation frequency, ω_m , matches the atom's Rabi frequency, Ω [18].¹ There are at least two different types of Rabi-resonance [13], and one of these finds application in a device called an atomic candle, in which field amplitude is locked to the peak of the Rabi-resonance in much the same way as field frequency is stabilized in an atomic clock [19], [20]. As discussed elsewhere [13], the atomic-candle signal has the form:

$$\delta_{\text{pop}} \sim \frac{\hbar^2 \omega_m \Omega^2 \gamma_2 \left[\gamma_2^2 + \left(\frac{\gamma_2}{\gamma_1} \right) \Omega^2 \right]^{-1}}{\sqrt{(\mu_B^2 B^2 - 4\hbar^2 \omega_m^2)^2 + 4\hbar^4 \gamma_1^2 \omega_m^2}}, \quad (1)$$

¹For the magnetic dipole transition considered here, $\Omega = \frac{\mu_B B}{\hbar}$, where μ_B is the Bohr magneton and B is the microwave magnetic field amplitude.

Manuscript received November 12, 2002; accepted September 10, 2003. This work was supported by U.S. Air Force Space and Missile Systems Center under Contract No. F040701-00-C-0009.

The authors are with the Electronics and Photonics Laboratory, The Aerospace Corporation, Los Angeles, CA 90009 (e-mail: james.c.camparo@aero.org).

B. Sickmiller also is with the School of Engineering and Applied Sciences, University of Virginia, Charlottesville, VA 22904.

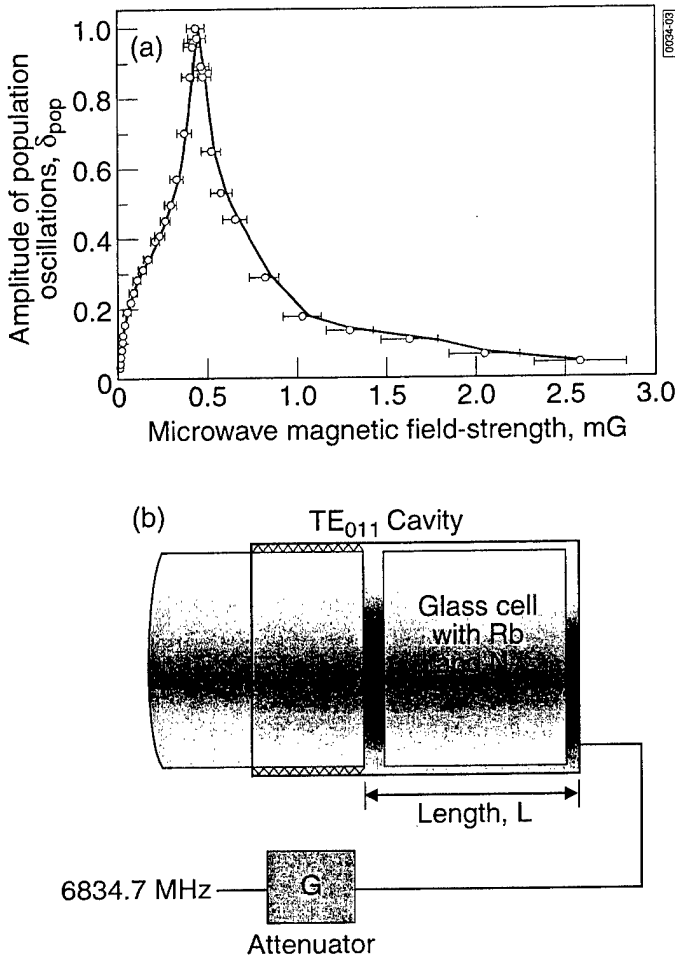


Fig. 1. (a) Example of an atomic-candle-type Rabi-resonance lineshape as used in the present experiment. Note that when the atoms experience a specific value of the microwave magnetic field strength, the amplitude of the modulation-induced atomic population oscillations increase dramatically. (b) Illustration of our use of the atomic-candle method to measure cavity resonance as discussed in the text. For different values of the cavity length, we measure the external gain required to tune the field back to the atoms' Rabi-resonance peak.

where γ_1 and γ_2 are the longitudinal and transverse atomic relaxation rates, respectively. This signal is illustrated in Fig. 1(a), in which experimental values of δ_{pop} are plotted as a function of the microwave magnetic field strength in our cavity. (Our method for measuring δ_{pop} will be discussed more fully later.) As Fig. 1(a) shows, there is a sharp resonant increase in δ_{pop} when $B = B_{res} = 2\hbar\omega_m/\mu_B$.² With regard to present considerations, Fig. 1(a) indicates that atoms can act as sensors of electromagnetic field strength via their atomic-candle signals; for a specific value of the modulation frequency, the maximum value of δ_{pop} occurs at a unique value of the cav-

²Because the field strength in the cavity varies linearly with the square root of the power fed into the cavity, we calibrated our external attenuator to field strength by taking advantage of the Rabi-resonance condition. Considering the attenuator as providing a fixed gain, G , to the microwave signal, $G_{res} \Rightarrow B_{res} \equiv 2\hbar\omega_m/\mu_B$, where G_{res} is the external attenuator setting (or gain) that gives rise to the Rabi-resonance peak.

ity's field strength.³ Fig. 1(b) illustrates how we used this idea to measure a microwave cavity's resonant frequency and quality factor. Briefly, for different values of the cavity length, we adjusted the external gain (i.e., attenuator) of the microwave signal in order to keep the microwave field strength in the cavity at the Rabi-resonance peak.

For an ideal cylindrical TE_{mnp} cavity mode excited by a fixed microwave frequency (e.g., the ground-state hyperfine transition frequency of Rb^{87} at 6834.7 MHz, $\omega_{hfs}/2\pi$), the field energy in the cavity, B^2 , can be written as [23]:

$$B^2 = \frac{\left(\frac{\omega_{hfs}}{2Q_c}\right)^2 B_o^2}{(L - L_{mnp})^2 \frac{(\pi pc)^4}{\omega_{hfs}^2 L_o^6} + \left(\frac{\omega_{hfs}}{2Q_c}\right)^2}, \quad (2)$$

where L is the cavity length; L_{mnp} is the specific length associated with the mnp-mode's resonance (for input frequency ω_{hfs}), and B_o^2 is the resonant field energy in the cavity. Note that B_o^2 is proportional to the setting of the external attenuator (expressed as a signal gain factor), G . Using a microwave field with relatively slow phase modulation (i.e., $\omega_m/2\pi = 10^2 - 10^3$ Hz), we induce atomic population oscillations; and, for a particular value of L , adjust the external gain to maximize the amplitude of the atomic population oscillations. Considering (1), we "tune" B (via the external gain) to the atomic-candle signal's peak. For this level of external gain, (1) indicates that $B(L) = 2\hbar\omega_m/\mu_B$, and we label this particular gain G_{res} . Because $B_o^2 \sim G$, we can rearrange (2) to yield:

$$\frac{1}{G_{res}} \sim \frac{\left(\frac{\mu_B}{2\hbar\omega_m}\right)^2 \left(\frac{\omega_{hfs}}{2Q_c}\right)^2}{(L - L_{mnp})^2 \frac{(\pi pc)^4}{\omega_{hfs}^2 L_o^6} + \left(\frac{\omega_{hfs}}{2Q_c}\right)^2}, \quad (3)$$

where we have approximated L_{mnp} with the nominal cavity length L_o in the factor that multiplies the cavity-length term in the denominator. Thus, a plot of G_{res}^{-1} as a function of L yields the cavity resonance lineshape and allows for a determination of L_{mnp} and Q_c . Not to belabor the point, (3) represents a local measure of the cavity's resonance, because the atoms in the cavity (frozen in place on the time scale of a Rabi period) sense the field strength in the particular region where the atomic-candle signal is generated and probed.

III. EXPERIMENTAL ARRANGEMENT

Fig. 2 shows a block diagram of our experimental arrangement. Light from a diode laser was tuned to the

³We note that our atomic-candle method is one of a several techniques developed to measure cavity characteristics using an atom's Rabi frequency; see for example [21]. Additionally, a number of years ago we developed a method for measuring local field strengths in a cavity using adiabatic rapid passage (ARP) [22]. However, due to the resonant nature of the atomic-candle signal, we believe the present method is more accurate than our previous ARP technique.

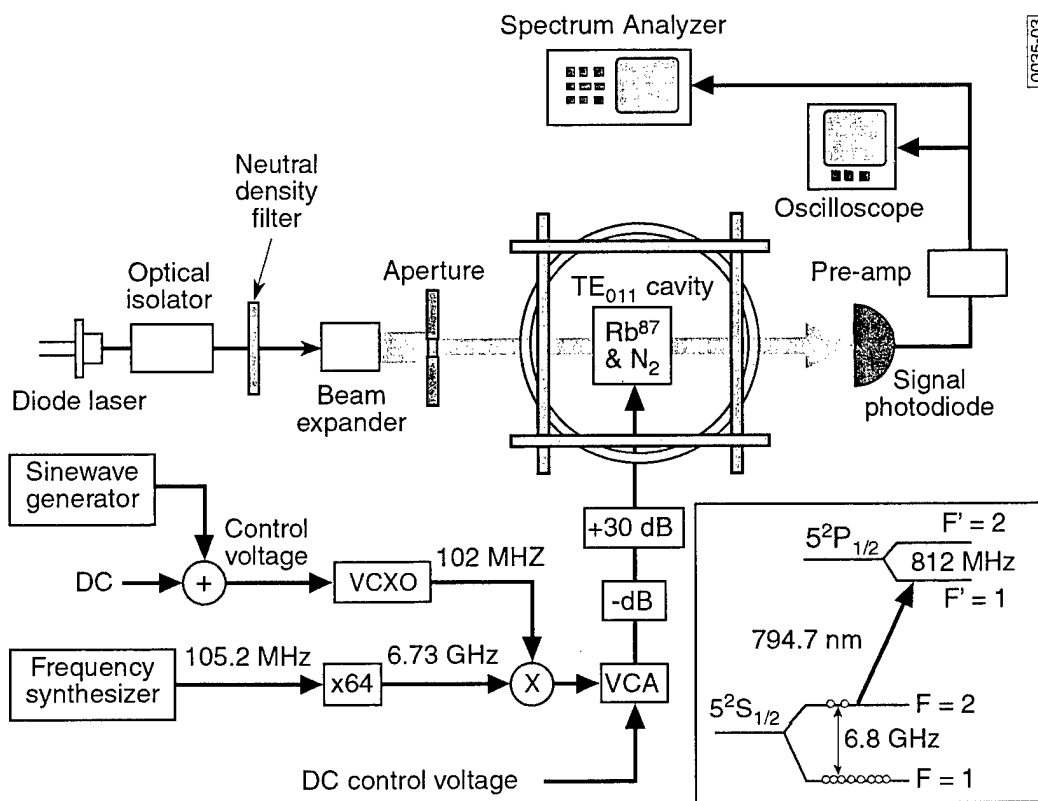


Fig. 2. Experimental arrangement.

Rb^{87} D_1 transition at 794.7 nm (i.e., $5^2S_{1/2}(F=2) - 5^2P_{1/2}(F'=1)$), attenuated by neutral density filters, then expanded and apertured to a final diameter of 0.8 cm with $I = 3.5 \mu\text{W}/\text{cm}^2$. (Given the 520 MHz Doppler broadening of the optical transition, we were just able to resolve the 812 MHz splitting between the $F'=1$ and $F'=2$ hyperfine states.) The laser beam passed into a resonance cell containing isotopically enriched Rb^{87} along with 10 torr N_2 , which was housed in a cylindrical TE_{011} microwave cavity nearly resonant with the ground-state hyperfine transition at 6834.7 MHz. The copper microwave cavity was constructed in two pieces, so a threaded end cap could be screwed in or out to change the cavity length.⁴ Radially, the 7070 glass resonance cell (Corning Inc., Corning, NY) fit snugly into the cavity. It had a length of ~ 5.6 cm (i.e., L_o) and a diameter, $2R$, of 5.7 cm; and it was heated with braided windings wrapped on the copper cavity body to about 35°C corresponding to a Rb vapor density of $\sim 6 \times 10^{10} \text{ cm}^{-3}$ [24]. The cavity and cell were centrally located in a set of three mutually perpendicular Helmholtz coils: two pairs zeroed out the Earth's residual magnetic field, and the third provided a quantization axis for the atoms (i.e., z-axis) parallel to the laser propagation direction and cavity symmetry axis: $B_{z,DC} \sim 400$ mG. Transmission of the light through the vapor was monitored with a Si photodiode.

⁴We measured the change in cavity length per cylinder turn, then checked that this was consistent with the documented threading of the end cap.

In the absence of microwaves resonant with the ($F=2$, $m_F=0$) - ($1,0$) hyperfine transition (i.e., 0-0 transition), depopulation optical pumping reduced the density of atoms in the $F=2$ absorbing state [25] and, consequently increased the amount of light transmitted through the vapor. However, when the resonant microwave signal was present, atoms returned to the $F=2$ state, thereby reducing the amount of transmitted light. The transmitted laser intensity thus acted as a measure of atomic population in the $F=2$ level, so any microwave-induced oscillation of this population was observed as oscillations in the transmitted light and appeared as a bright line on the spectrum analyzer. Because our atomic-candle signal is associated with population oscillations occurring at $2\omega_m$ [13], we were able to measure δ_{pop} very easily by simply recording the amplitude of the bright line on the spectrum analyzer at $2\omega_m$. We note that Doppler broadening played no role in our experiments as a consequence of Dicke narrowing [26], [27].

The microwaves were derived from a very low phase-noise frequency synthesizer (i.e., -63 dBc from 0.5 Hz to 15 kHz) whose output at 105.2 MHz was multiplied up into the microwave regime then mixed with the output of a voltage-controlled crystal oscillator (VCXO) at ~ 102 MHz. The microwaves were attenuated by the combination of a voltage-controlled attenuator (VCA) and a fixed attenuator (labeled as $-dB$ in Fig. 2) before being amplified by a $+30$ dB solid-state amplifier. A sinusoidal signal of frequency ω_m was added to a direct cur-

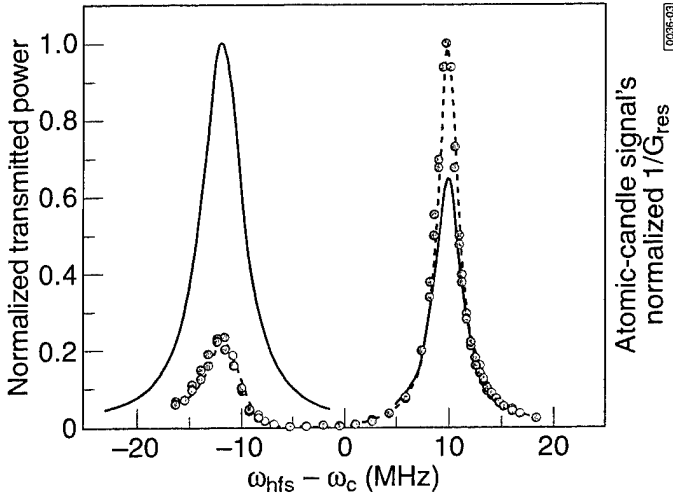


Fig. 3. Cavity resonances as a function of $\Delta_c \equiv \omega_{\text{hfs}} - \omega_c$. The solid line corresponds to the cavity resonance observed using the traditional power-transmission technique. The circles correspond to the cavity resonance as observed using the atomic-candle method. As discussed in the text, the difference between these two curves is due to the local nature of the atomic-candle method as opposed to the global nature of the power-transmission method.

rent (DC) voltage in order to provide the VCXO's control voltage, V_c . The DC level of V_c tuned the average microwave frequency to the 0-0 hyperfine resonance, and the sine wave provided microwave frequency (i.e., phase, $\delta\theta$) modulation: $\delta\theta(t) = m \cos(\omega_m t)$. In these experiments, $\omega_m/2\pi = 328$ Hz and the modulation index, m , of the microwaves was 0.74.

Prior to measuring the cavity resonance with the atomic-candle signal, we studied the cavity with a more traditional power-transmission technique. Briefly, we used a directional coupler to measure the reflected microwave power from the cavity as a function of length, $P_r(L)$; then, defining P_o as the reflected power with the cavity off resonance, we approximated the transmitted power, $P_t(L)$, as the difference between P_o and $P_r(L)$. The solid line in Fig. 3 shows this transmitted power as a function of the cavity's detuning, Δ_c , from the 0-0 hyperfine resonant frequency. Basically, Δ_c is a parameter that re-expresses the cavity's length in terms of an appropriate cavity resonant frequency for that length:

$$\Delta_c \equiv \omega_{\text{hfs}} - c \sqrt{\left(\frac{x'_{mn}}{R}\right)^2 + \left(\frac{\pi p}{L}\right)^2} = \omega_{\text{hfs}} - \omega_c, \quad (4)$$

where L is the measured cavity length, and x'_{mn} is the n th root of $J'_m(x) = 0$ with J'_m the derivative of an m th order Bessel function [23]. For the TE_{011} mode, $x'_{mn} = 3.832$ and $p = 1$.

As Fig. 3 clearly shows, our cavity exhibits two resonances near 6.8 GHz separated by about 22 MHz.⁵ The lower frequency resonance (i.e., $\Delta_c < 0$) has a Q_c of ~ 1500 ,

⁵For illustrative purposes, we have chosen the zero of Δ_c so that the two cavity resonances appear nearly symmetrical about $\Delta_c = 0$.

and the higher frequency resonance has a Q_c of ~ 2200 . Moreover, the larger amplitude of the low-frequency resonance implies that it is better able to couple microwave power into the cavity. In a separate set of experiments, in which we examined the cavity without the resonance cell using the reflected power technique, we also observed these two resonances. For the empty cavity measurements, we fixed the cavity length, scanned the input microwave frequency as we measured the reflected power, and thereby determined the resonant frequency for each of the modes at the specific cavity length. Repeating this procedure for a set of cavity lengths, we then fit the square of the resonant frequencies to $c^2 \left[\left(\frac{x'_{mn}}{R} \right)^2 + \left(\frac{\pi p}{L} \right)^2 \right]$, and obtained x'_{mn} and p values for each of the modes. We found that both cavity resonances were consistent with the TE_{011} parameters: for the lower frequency resonance we found $x'_{mn} = 3.769 \pm 0.016$ and $p = 1.04 \pm 0.02$ and for the higher frequency resonance we found $x'_{mn} = 3.821 \pm 0.015$ and $p = 1.01 \pm 0.02$.

Because we probe the atoms' 0-0 hyperfine transition, angular momentum conservation implies that we are sensitive only to the z-component of the microwave's magnetic field, which is defined by our Helmholtz coil's DC magnetic field to be parallel to the cavity axis. Consequently, for an ideal cavity, we should be relatively insensitive to the cavity's transverse magnetic (TM) modes. However, the 1.1-cm diameter holes in our cavity, which allow the laser light to enter and exit the cavity (as well as the microwave antenna within the cavity), perturb the cavity geometry and will cause a coupling of cavity modes. Due to the degeneracy of the TE_{011} and TM_{111} modes, it, therefore, is likely that the two modes we observe are actually "hybrid" cavity modes representing a superposition of the pure TE_{011} and TM_{111} modes. Because angular momentum conservation indicates that we would be sensitive only to the TE_{011} component of these hybrid modes, for future reference and simplicity we will refer to the low-frequency hybrid as the TE_{011}^a mode and the higher-frequency hybrid as the TE_{011}^b mode.

Returning to the cavity experiments with the resonance cell, circles in Fig. 3 show our measurements of G_{res}^{-1} as a function of $\Delta_c = \omega_{\text{hfs}} - \omega_c$ using the atomic-candle method. Similar to the reflected power measurements, we see two modes with the same widths and spacing.⁶ The striking difference between these two measurement procedures is the asymmetry in the TE_{011}^a and TE_{011}^b modes' amplitudes. Specifically for the atomic-candle method, it appears that less gain is required by the TE_{011}^b mode in order to produce a given value of cavity field strength, implying that this mode is better able to couple microwaves into the cavity. This observation would seem to be at odds with the results from the power-transmission method. To resolve this discrepancy, we note that the laser only probes atoms very near the cavity axis (i.e., $R = 2.9$ cm,

⁶Using the atomic-candle method, $Q_c \sim 1700$ for the TE_{011}^a mode, and $Q_c \sim 2700$ for the TE_{011}^b .

$r_{\text{laser}} = 0.4$ cm), and that the atomic-candle method provides a local determination of the cavity's modal features, specifically the z-component of the microwave magnetic field strength. Consequently, though the TE_{011}^a mode is globally more efficient at coupling power into the cavity, the TE_{011}^b mode appears more efficient at localizing the axial component of the microwave magnetic field in the central regions of the cavity in which the atoms are probed. Here then, we have a rather serendipitous and dramatic demonstration of the atomic-candle method's utility for cavity resonance measurements. Specifically, when coupled with a more traditional method, the local nature of the atomic-candle method can "tease out" information on a cavity mode's spatial profile.

IV. TEMPORAL VARIATIONS OF THE CAVITY'S RESONANT FREQUENCY AND QUALITY FACTOR

As suggested in Section I, our primary motivation for initiating these studies was to investigate temporal changes in the resonant frequency and quality factor of a gas-cell atomic clock's microwave cavity. We hypothesized that, due to a slow redistribution of alkali metal within the resonance cell over long periods of time, Q_c and/or ω_c might "age." To test this hypothesis, we removed our glass resonance cell from the cavity, and "drove down" the rubidium condensed phase to one end of the cell.⁷ Briefly, we wrapped heating wire around the sides and top of the cell and heated this to about 60°C; additionally, we placed heat-sink putty on the cell's "pull-off" tip (i.e., the small cylindrical protrusion to which the cell had been attached to a vacuum system during its fabrication) and connected this to a metal table separated from the rest of the cell by foam. We cooled the table down by placing dry ice on it; and we were able to obtain a temperature gradient across the cell of something close to 140°C, which we maintained for ~12 hours. After the dry ice evaporated, the temperature gradient across the cell was roughly 40°C. The condensed phase must move to the cell's cold point for a vapor in equilibrium with the condensed phase, and we assumed that after 60 hours nearly all of the Rb had collected in our cell's tip.⁸

Following the drive-down procedure, we placed the resonance cell in the cavity, heated the cell to 35°C, and began a series of measurements on the TE_{011}^b mode's resonant frequency and Q . These are shown in Fig. 4 by the open triangles and circles, respectively. Although we saw no change in the mode's resonant frequency, there was a very noticeable change in the cavity mode's Q . The solid line is a least squares fit of the data to an exponential form:

$$Q_c(t) = Q_o + \delta Q e^{-\frac{t}{\tau}}, \quad (5)$$

⁷Prior to this drive-down procedure, the cavity and resonance cell had been maintained at 62°C for nearly a week.

⁸Though we could not observe a liquid phase of the alkali in our cell (there was too little isotopically enriched rubidium in the relatively large cell for easy visualization), we knew that a condensed phase must exist because the Rb vapor density in our cell depended on temperature as expected for a liquid/vapor equilibrium.

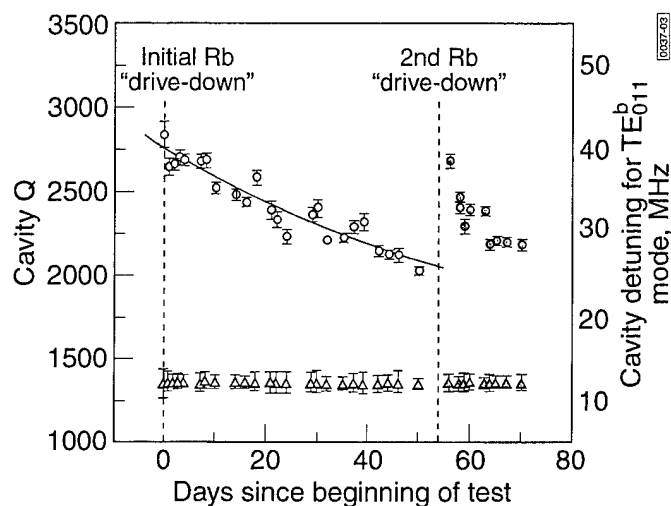


Fig. 4. Cavity- Q and resonant-frequency aging in our microwave cavity. Open symbols correspond to data following the first drive down. Filled symbols correspond to data following the second drive down. Circles correspond to cavity- Q , and triangles correspond to the cavity's resonant frequency.

and we find $Q_o = 1495$, $\delta Q = 1255$, and $\tau = 67$ days. At day 52, we halted the experiment, removed the resonance cell from the cavity, and repeated the exact same drive-down procedure. We then placed the resonance cell back in the cavity at 35°C and continued our measurements of the TE_{011}^b mode's resonant frequency and quality factor; these are shown as filled triangles and circles, respectively, in Fig. 4. As the data clearly show, although the resonant frequency was unaffected by the second drive down, the cavity- Q recovered to its initial value.

We hypothesize that the cavity- Q 's decay is due to a redistribution of condensed phase Rb within the resonance cell, perhaps in the form of a film coating the inside glass surface. Several lines of argument lead us to this conclusion. First, whatever the mechanism responsible for the cavity- Q 's decay, it cannot be associated with a change in the electrical dimensions of the cavity/resonance cell; otherwise, the cavity detuning corresponding to the TE_{011}^b mode would have changed during the course of the experiment. Furthermore, because we had observed that the cavity- Q depended on the placement of the resonance cell within the cavity, at one point we were tempted to explain the decay as arising from resonance-cell "creep" within the cavity (i.e., over a period of days, the resonance cell might undergo a mechanical relaxation of its position within the cavity). However, for each data point shown in Fig. 4, we obtained the TE_{011}^b mode lineshape by increasing the cavity length from "zero," which corresponded to the cavity ends just touching the glass resonance cell. This had the effect of repositioning the resonance cell in the cavity for each of the data points, thereby eliminating any effect of creep over the long-term test. In fact, we believe that some of the variability among the data points shown in Fig. 4 may be due to this repositioning. Finally, the cavity- Q 's recovery to its initial value following the second drive down argues forcefully for an alkali redistribution effect. Even

the relatively fast (i.e., $\tau \sim 10$ days) cavity-Q decay after the second drive down is consistent with the evolution of an alkali film. Because surface diffusion coefficients can change by orders of magnitude, depending on the relative surface coverage [28], it is not difficult to imagine that there were differences in the initial surface coverage following the first and second drive-down procedures given the differences in the resonance-cell's history in the two cases. We also note that the anticipated time scale for cavity-Q degradation due to film evolution is consistent with our findings: given that surface diffusion coefficients can be on the order of 10^{-5} cm²/s,⁹ our resonance cell surface area of 10^2 cm² would imply a multimonth time constant for complete coverage.

V. CONSEQUENCES FOR GAS-CELL CLOCK FREQUENCY AGING

As already mentioned, changes in the cavity-Q of a gas-cell clock will affect the clock's frequency as a result of the position-shift and/or cavity-pulling effects. In this Section, we want to estimate the magnitude of these effects for a clock based on the present experiment's TE_{011}^b mode. Although we recognize that our cavity-Q is roughly a factor of 5 to 10 times larger than that of typical clocks, the present exercise nonetheless has merit as it places an upper bound on the frequency variations that might occur in these devices. As shown below, this upper bound is actually quite large, and it suggests that cavity-Q variations may play a role in the long-term stability of Rb atomic clocks.

According to Sarosy *et al.* [32], the position-shift effect's dependence on microwave power in commercial Rb frequency standards can be as large as 3×10^{-11} /dB. However, physical considerations lead us to expect the position shift to depend not so much on the input power, P , but on the energy density, E , within the cavity. Therefore, we expand the atomic clock's frequency, ω_{clk} , in a Taylor series about the nominal cavity energy density, E_0 , to obtain $\delta\omega_{\text{clk}} = \left. \frac{\partial\omega_{\text{clk}}}{\partial E} \right|_{E=E_0} \delta E$. Because the energy density scales like $Q_c P$, $\delta E \sim Q_c \delta P + P \delta Q_c$, and so the fractional change in the position shift due to a microwave power or cavity-Q variation, $\delta[\Delta y_{\text{position}}]$, may be written as:

$$\delta[\Delta y_{\text{position}}] = \left. \frac{E_0}{\omega_{\text{clk}}} \frac{\partial\omega_{\text{clk}}}{\partial E} \right|_{E=E_0} \left(\frac{\delta P}{P_c} + \frac{\delta Q}{Q_c} \right). \quad (6)$$

Based on the results of Sarosy *et al.* [32], a 0.23 relative change in microwave power can give rise to a 3×10^{-11} fractional frequency change, implying that $\left. \frac{E_0}{\omega_{\text{clk}}} \frac{\partial\omega_{\text{clk}}}{\partial E} \right|_{E=E_0} = 1.3 \times 10^{-10}$. Thus, we expect $\delta[\Delta y_{\text{position}}] \sim 10^{-10}(\delta Q/Q_c)$.

The fractional frequency shift due to cavity pulling can be written as $\Delta y_{\text{pull}} = \frac{\alpha Q_c (\omega_c - \omega_{\text{hfs}})}{\omega_{\text{hfs}} Q_a (1+S)}$, where α is a parameter representing the degree of coupling between the atoms

and the cavity, S is a saturation parameter, and Q_a is the atoms' quality factor [3], [6]. In gas-cell clocks, $\alpha \sim 10^{-2}$, $S \sim 2$, and $Q_a \sim 10^7$; thus, for a relative cavity detuning on the order of Q_c^{-1} , $\delta[\Delta y_{\text{pull}}] \sim 3 \times 10^{-10}(\delta Q/Q_c)$. Thus, the position-shift and cavity-pulling effects can be of the same order of magnitude; therefore, we express the upper bound on frequency aging due to cavity-Q variations as:

$$\frac{\delta\omega_{\text{clk}}(t)}{\omega_{\text{clk}}} \sim 4 \times 10^{-10} \frac{\delta Q(t)}{Q_c}. \quad (7)$$

Substituting from (5), we get a cavity-Q induced, frequency-aging rate of roughly 3×10^{-12} /day at short times t , just after a clock's turn-on. This is of the same order of magnitude as a recent measurement of initial frequency aging in a high-quality Rb clock onboard a geosynchronous satellite, and more than an order-of-magnitude larger than the clock's eventual quiescent frequency-aging rate [33].

VI. SUMMARY

We have used an atomic-candle signal to investigate the long-term aging of a gas-cell clock's microwave cavity; and for the first time, we have obtained evidence pointing to a role for alkali redistribution (within the resonance cell) in the gas-cell clock's frequency stability. Additional work in this area is certainly warranted. In particular, there is a lack of knowledge regarding alkali surface diffusion on various types of glass; and, given the present findings, this could be a very fruitful area of investigation. Moreover, we have found that, when our atomic-candle method is combined with more traditional methods, the combination has the potential to yield information on spatial mode profiles within the cavity. Consequently, although we have used the atomic-candle method to investigate cavity resonances in the specific case of the rubidium atomic clock, we believe that the method will have much wider applicability.

ACKNOWLEDGMENTS

The authors thank A. Presser for assistance in performing some of the experiments, and S. Moss for stimulating discussions regarding surface diffusion.

REFERENCES

- [1] A. Risley and G. Busca, "Effect of line inhomogeneity on the frequency of passive Rb⁸⁷ frequency standards," in *Proc. 32nd Annu. Symp. Freq. Contr.*, 1978, pp. 506-513.
- [2] A. Risley, S. Jarvis, and J. Vanier, "The dependence of frequency upon microwave power of wall-coated and buffer-gas-filled gas cell Rb⁸⁷ frequency standards," *J. Appl. Phys.*, vol. 51, no. 9, pp. 4571-4576, 1980.
- [3] J. Vanier and C. Audoin, *The Quantum Physics of Atomic Frequency Standards*, vol. 2, Bristol, Great Britain: Adam Hilger, 1989, pp. 1205-1211.
- [4] J. C. Camparo, "A partial analysis of drift in the rubidium gas cell atomic clock," in *Proc. 18th Annu. Precise Time and Time Interval (PTTI) Applications and Planning Meeting*, 1986, pp. 565-588.

⁹See for example [29], [30], [31].

- [5] W. J. Riley, "The physics of the environmental sensitivity of rubidium gas cell atomic frequency standards," in *Proc. 22nd Annu. Precise Time and Time Interval (PTTI) Applications and Planning Meeting*, 1990, pp. 441–452.
- [6] J. Viennet, C. Audoin, and M. Desaintfussien, "Cavity pulling in passive frequency standards," *IEEE Trans. Instrum. Meas.*, vol. IM-21, no. 3, pp. 204–209, 1972.
- [7] X. Huang, B. Xia, D. Zhong, S. An, X. Zhu, and G. Mei, "A microwave cavity with low temperature coefficient for passive rubidium frequency standards," in *Proc. IEEE Int. Freq. Contr. Symp. PDA Exhibition*, 2001, pp. 105–107.
- [8] H. E. Williams, T. M. Kwon, and T. McClelland, "Compact rectangular cavity for rubidium vapor cell frequency standards," in *Proc. 37th Annu. Symp. Freq. Contr.*, 1983, pp. 12–17.
- [9] E. Eltsufin, A. Stern, and S. Fel, "Compact rectangular-cylindrical cavity for rubidium frequency standard," in *Proc. 45th Annu. Symp. Freq. Contr.*, 1991, pp. 567–571.
- [10] J. Deng, "Subminiature microwave cavity for atomic frequency standards," in *Proc. IEEE Int. Freq. Contr. Symp. PDA Exhibition*, 2001, pp. 85–88.
- [11] L. B. Young, "Frequency measurements," in *Technique of Microwave Measurements*. C. G. Montgomery, Ed. New York: McGraw-Hill, 1947, pp. 343–407.
- [12] J. C. Camparo, "Magnetic resonance in cesium vapor: Detection of photoinduced paramagnetic species and spin exchange amplification of rf broadening," Ph.D. dissertation, Columbia University, New York, NY, 1981.
- [13] J. G. Coffer, B. Sickmiller, A. Presser, and J. C. Camparo, "Line shapes of atomic-candle-type Rabi resonances," *Phys. Rev. A*, vol. 66, pp. 023806-1–023806-7, 2002.
- [14] T. Swan-Wood, J. G. Coffer, and J. C. Camparo, "Precision measurements of absorption and refractive-index using an atomic candle," *IEEE Trans. Instrum. Meas.*, vol. 50, no. 5, pp. 1229–1233, 2001.
- [15] E. L. Ginzton, *Microwave Measurements*. New York: McGraw-Hill, 1957, pp. 391–434.
- [16] U. Cappeller and H. Mueller, "Phase modulated excitation on optically pumped spin system," *Ann. der Phys.*, vol. 42, no. 3, pp. 250–264, 1985.
- [17] R. P. Frueholz and J. C. Camparo, "Entropy and attractor dimension as measures of the field-atom interaction," *Phys. Rev. A*, vol. 47, no. 3, pp. 4404–4411, 1993.
- [18] J. C. Camparo and J. G. Coffer, "Accessing photon number via an atomic time interval," *Phys. Rev. A*, vol. 66, pp. 043416-1–043416-4, 2002.
- [19] J. C. Camparo, "Atomic stabilization of electromagnetic field strength using Rabi resonances," *Phys. Rev. Lett.*, vol. 80, no. 2, pp. 222–225, 1998.
- [20] J. G. Coffer and J. C. Camparo, "Atomic stabilization of field intensity using Rabi resonances," *Phys. Rev. A*, vol. 62, pp. 013812-1–013812-9, 2000.
- [21] C. Fertig and K. Gibble, "Laser-cooled ^{87}Rb clock," *IEEE Trans. Instrum. Meas.*, vol. 48, no. 2, pp. 520–523, 1999.
- [22] R. P. Frueholz and J. C. Camparo, "Microwave field strength measurement in a rubidium clock cavity via adiabatic rapid passage," *J. Appl. Phys.*, vol. 57, no. 3, pp. 704–708, 1985.
- [23] J. D. Jackson, *Classical Electrodynamics*. New York: Wiley, 1975, pp. 334–390.
- [24] T. J. Killian, "Thermionic phenomena caused by vapors of rubidium and potassium," *Phys. Rev.*, vol. 27, pp. 578–587, 1926.
- [25] W. Happer, "Optical pumping," *Rev. Mod. Phys.*, vol. 44, no. 2, pp. 169–249, 1972.
- [26] R. H. Dicke, "The effect of collisions upon the Doppler width of spectral lines," *Phys. Rev.*, vol. 89, no. 2, pp. 472–473, 1953.
- [27] R. P. Frueholz and C. H. Volk, "Analysis of Dicke narrowing in wall-coated and buffer-gas-filled atomic storage cells," *J. Phys. B: At. Mol. Phys.*, vol. 18, pp. 4055–4067, 1985.
- [28] A. G. Naumovets and Z. Zhang, "Fidgety particles on surfaces: How do they jump, walk, group, and settle in virgin areas," *Surf. Sci.*, vol. 500, pp. 414–436, 2002.
- [29] S. Garofalini, "Potassium diffusion at the surface of a $\text{K}_2\text{O} \cdot 3\text{SiO}_2$ glass," *J. Vac. Sci. Technol. A*, vol. 2, pp. 79–81, 1984.
- [30] A. P. Graham and J. P. Toennies, "Macroscopic diffusion and low-frequency vibrations of sodium on Pt(111) investigated with helium atom scattering," *J. Phys. Chem. B*, vol. 105, pp. 4003–4009, 2001.
- [31] P. S. Maiya and J. M. Blakely, "Surface self-diffusion and surface energy of nickel," *J. Appl. Phys.*, vol. 38, no. 2, pp. 698–704, 1967.
- [32] E. B. Sarosy, W. A. Johnson, S. K. Karuza, and F. Voit, "Measuring frequency changes due to microwave power variations as a function of C-field setting in a rubidium frequency standard," in *Proc. 23rd Annu. Precise Time and Time Interval (PTTI) Applications and Planning Meeting*, 1991, pp. 229–235.
- [33] J. G. Coffer and J. C. Camparo, "Long-term stability of a rubidium atomic clock in geosynchronous orbit," in *Proc. 31st Annu. Precise Time and Time Interval (PTTI) Systems and Applications Meeting*, 2000, pp. 65–74.

LABORATORY OPERATIONS

The Aerospace Corporation functions as an "architect-engineer" for national security programs, specializing in advanced military space systems. The Corporation's Laboratory Operations supports the effective and timely development and operation of national security systems through scientific research and the application of advanced technology. Vital to the success of the Corporation is the technical staff's wide-ranging expertise and its ability to stay abreast of new technological developments and program support issues associated with rapidly evolving space systems. Contributing capabilities are provided by these individual organizations:

Electronics and Photonics Laboratory: Microelectronics, VLSI reliability, failure analysis, solid-state device physics, compound semiconductors, radiation effects, infrared and CCD detector devices, data storage and display technologies; lasers and electro-optics, solid-state laser design, micro-optics, optical communications, and fiber-optic sensors; atomic frequency standards, applied laser spectroscopy, laser chemistry, atmospheric propagation and beam control, LIDAR/LADAR remote sensing; solar cell and array testing and evaluation, battery electrochemistry, battery testing and evaluation.

Space Materials Laboratory: Evaluation and characterizations of new materials and processing techniques: metals, alloys, ceramics, polymers, thin films, and composites; development of advanced deposition processes; nondestructive evaluation, component failure analysis and reliability; structural mechanics, fracture mechanics, and stress corrosion; analysis and evaluation of materials at cryogenic and elevated temperatures; launch vehicle fluid mechanics, heat transfer and flight dynamics; aerothermodynamics; chemical and electric propulsion; environmental chemistry; combustion processes; space environment effects on materials, hardening and vulnerability assessment; contamination, thermal and structural control; lubrication and surface phenomena. Microelectromechanical systems (MEMS) for space applications; laser micromachining; laser-surface physical and chemical interactions; micropropulsion; micro- and nanosatellite mission analysis; intelligent microinstruments for monitoring space and launch system environments.

Space Science Applications Laboratory: Magnetospheric, auroral and cosmic-ray physics, wave-particle interactions, magnetospheric plasma waves; atmospheric and ionospheric physics, density and composition of the upper atmosphere, remote sensing using atmospheric radiation; solar physics, infrared astronomy, infrared signature analysis; infrared surveillance, imaging and remote sensing; multispectral and hyperspectral sensor development; data analysis and algorithm development; applications of multispectral and hyperspectral imagery to defense, civil space, commercial, and environmental missions; effects of solar activity, magnetic storms and nuclear explosions on the Earth's atmosphere, ionosphere and magnetosphere; effects of electromagnetic and particulate radiations on space systems; space instrumentation, design, fabrication and test; environmental chemistry, trace detection; atmospheric chemical reactions, atmospheric optics, light scattering, state-specific chemical reactions, and radiative signatures of missile plumes.